Supersaturation Development in a Vertical-Flow Thermal Diffusion Chamber

P. C. MAHATA, D. J. ALOFS AND A. M. SINNARWALLA

Dept. of Mechanical and Aerospace Engineering and Graduate Center for Cloud Physics Research, University of Missouri-Rolla

(Manuscript received 13 April 1973, in revised form 7 July 1973)

ABSTRACT

Analytical expressions are derived for temperature and vapor pressure profiles in a vertical-plate, steady-flow, thermal diffusion chamber designed to count cloud condensation nuclei. The influence of longitudinal diffusion of heat and water vapor on the supersaturation rise time is shown to be quite significant at low sample velocities. The effect of different velocity profile shapes is also investigated.

1. Introduction

A vertical-plate, steady-flow, thermal diffusion chamber designed to count cloud condensation nuclei has been developed and is described in an earlier paper (Sinnarwalla and Alofs, 1973). The earlier paper indicates that, at any given supersaturation, the vertical chamber can provide eight times more growth time than is available in the conventional horizontal plate chamber. The earlier paper also shows that this additional growth time allows the vertical chamber to be used at lower supersaturations than can the horizontal chamber.

The scope of the present paper is narrower than that of the earlier one. We now wish to investigate the supersaturation development in such chambers. The major results of the analyses will be applicable to either horizontal or vertical steady-flow chambers, with arbitrary plate spacing. Some of the supportive calculations will, however, require fixing various parameters; and, for these calculations, attention will be focused on the chamber described in the earlier paper.

Consider, then, a chamber featuring steady laminar flow of the sample downward between two vertical plates, each 100 cm long by 13.2 cm wide, with a plate spacing (d) of 1 cm (Fig. 1). One plate is kept at a temperature T_h, the hot plate temperature, the other at temperature T_c, the cold plate temperature. For the entire length of the cold plate, and for the lower 85 cm length of the hot plate, the inside plate surfaces are covered with filter paper which is continually supplied with water. Water is not supplied to the upper length (z_0, 15 cm) of the hot plate, however, in order to avoid the transient supersaturations described by Fitzgerald (1970) and by Saxena *et al.* (1970).

The sample enters the chamber at relative humidity ϕ, expressed in fractional form, and at temperature T_{in}. When $T_{in}<T_h$, the z_0 region of the hot plate remains dry, and we will show that the available growth time is then relatively insensitive to T_{in} and ϕ. When $T_{in}>T_h$, the z_0 region on the hot plate may be condensed

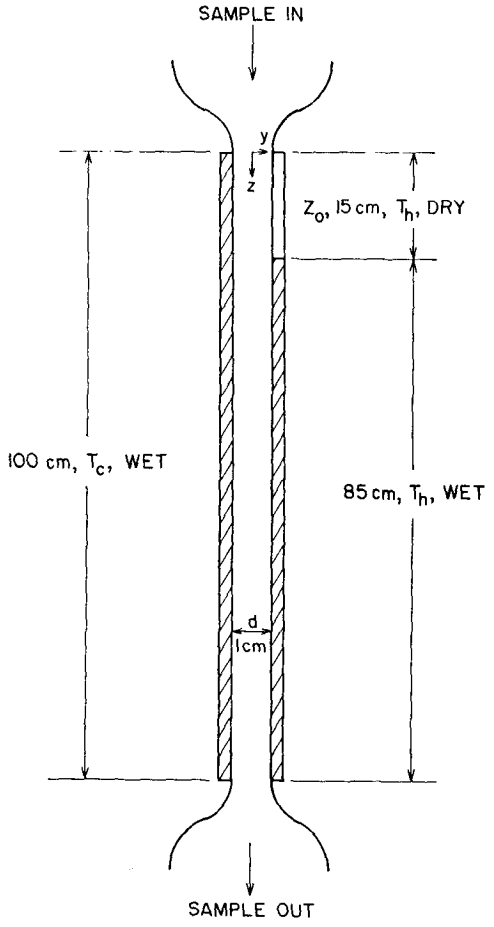

FIG. 1. Schematic of the steady-flow, vertical-plate thermal diffusion chamber.

upon for some values of ϕ. For $T_{in}-T_h<5$C, this latter case does not cause a transient supersaturation, because water vapor diffuses to the hot plate more quickly than does the heat. Using $T_{in}>T_h$ does, however, cause uncertainty as to whether or not the z_0 region on the hot plate is wet or dry, and hence causes uncertainty in the available growth time. Therefore, for simplicity in the following analysis, the z_0 region of the hot plate will be assumed dry.

As the sample flows through the chamber, the local temperature (T) and water vapor pressure (p) eventually become linearly proportional to the distance from the cold plate. This produces the same approximately parabolic supersaturation profile which occurs in the conventional static, or zero flow, thermal diffusion chamber. The supersaturation midway between the plates is the operating supersaturation S_M, and is given by the following approximate relation from the earlier paper:

$$S_M=(T_h-T_c)^2/25, \tag{1}$$

where S_M is in percent and (T_h-T_c) in degrees Celsius. This result is independent of plate spacing but is most accurate for $T_h=25$C and $S_M<5\%$.

One other result from the earlier paper is also now summarized for later use. In order to avoid a buoyancy-induced backflow near the hot plate, the sample velocity must be kept larger than

$$V_c=0.43(T_h-T_c)d^2, \tag{2}$$

where V_c is the centerline velocity (cm sec^{-1}); that is, V_c is the sample velocity at $y=0$. The term (T_h-T_c) is again in degrees Celsius while the plate spacing d is in centimeters.

2. Temperature profile

Local supersaturation S is defined by

$$S=[p/p_e(T)]-1, \tag{3}$$

where $p_e(T)$ is the equilibrium vapor pressure of water at the local temperature T. Thus, to determine supersaturations in the developing region of the chamber, temperature and vapor distributions must be found.

The problem is treated as two dimensional since three-dimensional calculations for the fully developed region of a chamber having plate spacing d and width $13d$ indicate that a two-dimensional solution applies accurately over the middle $8d$ wide region of the $13d$ wide chamber. The governing differential equation for temperature is

$$u\frac{\partial T}{\partial z}=\alpha\left(\frac{\partial^2 T}{\partial y^2}+\frac{\partial^2 T}{\partial z^2}\right), \tag{4}$$

where u and α are flow velocity and thermal diffusivity, respectively, for the fluid. The fluid velocity u is taken to be uniform, which constitutes the "slug flow" assumption. It is to be noted that the last term in (4) accounts for the longitudinal diffusion of heat.

The following boundary conditions are imposed:

$$\left.\begin{aligned} &T(-d/2,z)=T_c\\ &T(d/2,z)=T_h\\ &T(y,0)=T_{in}\\ &T(y,\infty)\text{ is finite}\end{aligned}\right\}. \tag{5}$$

The solution to (4) and (5) was found using separation of variable techniques. Many examples of this technique may be found in Carslaw and Jaeger (1959) among others. Thus, the solution for the temperature field is

$$T(y,z)=\tfrac{1}{2}(T_h+T_c)+(T_h-T_c)y/d+(T_h-T_c)$$
$$\times\sum_{n=1,2,\ldots}^{\infty}F_n\exp\{-(z/d)[(n^2\pi^2+\mathrm{Pe}^2/4)^{\frac{1}{2}}-\mathrm{Pe}/2]\}$$
$$\times\sin\{n\pi(y/d+\tfrac{1}{2})\}, \tag{6}$$

where

$$F_n=\frac{2}{n\pi}\{[(T_{in}-T_c)/(T_h-T_c)][1-(-1)^n]+(-1)^n\},$$

and where

$$\mathrm{Pe}=ud/\alpha.$$

3. Vapor pressure profile for $z<z_0$

The vapor diffusion problem occurring in the region $z<z_0$ is governed by the differential equation

$$u\frac{\partial p}{\partial z}=D\left(\frac{\partial^2 p}{\partial y^2}+\frac{\partial^2 p}{\partial z^2}\right), \tag{7}$$

where D is the diffusivity of water vapor in air. In (7) the Soret effect has been neglected. This simplification is justified for small temperature gradients (Fitzgerald, 1972).

The boundary conditions are

$$\left.\begin{aligned} &p(-d/2,z)=p_c\\ &\frac{\partial p}{\partial y}(d/2,z)=0\quad\text{or}\quad p(3d/2,z)=p_c\\ &p(y,0)=\phi p_{in}\\ &p(y,\infty)=p_c\end{aligned}\right\}, \tag{8}$$

where p_c and p_{in} are the equilibrium vapor pressures of water at temperatures T_c and T_{in}, respectively. The reason the second boundary condition in (8) can be expressed in the two ways shown is that the present problem is equivalent to one in which the hot dry wall is replaced by a cold wet wall located at a distance $2d$ from the cold plate (Fig. 1). In the second problem,

symmetry dictates a zero derivative at $y=d/2$. The second problem has been solved by Schneider (1957) with the following result:

$$p(y,z)=p_c+2(\phi p_{in}-p_c)\sum_{n=0,1,2,\ldots}^{\infty}(\mu_n \sin\mu_n)^{-1}\times\exp\{-(z/2d)[4\mu_n^2+\mathrm{Pa}^2)^{\frac{1}{2}}-\mathrm{Pa}]\}\times\cos[2\mu_n(y/2d-\tfrac{1}{4})], \quad (9)$$

where

$$\mu_n=(2n+1)\pi/2,$$

and where

$$\mathrm{Pa}=ud/D.$$

4. Vapor pressure profile for $z>z_0$

Eq. (7) serves as the governing equation for vapor diffusion in the region $z>z_0$. The following boundary conditions are used:

$$\left.\begin{aligned} &p(-d/2,z)=p_c\\ &p(d/2,z)=p_h\\ &p(y,z_0)=p^*\\ &p(y,\infty)\text{ is finite}\end{aligned}\right\}, \quad (10)$$

where p_h is the equilibrium vapor pressure of water at temperature T_h, and p^* is for simplicity taken to be a constant. The value of p^* is obtained from the solution of the $z<z_0$ region and is taken to be the minimum value of $p(y,z_0)$. Thus, p^* is $p(d/2,z_0)$ from Schneider's solution, i.e., from (9).

The solution of (7) and (10) is mathematically analogous to the solution of (4) and (5) and is thus found in (6) by substituting p, D, p_c, p_h and p^* for T, α, T_c, T_h and T_{in}, respectively.

5. Supersaturation development

In the present application only the nuclei near the centerline ($y=0$) are counted; therefore, the supersaturation histories of these nuclei are of prime interest. These supersaturation histories can be described by a time interval t_R in which the supersaturation is rising. Thereafter, until the nuclei reach the exit of the chamber, the supersaturation is virtually constant with a value given by (1). To be more explicit, let t_R, the rise time, be defined to begin when a nucleus enters the region $z>z_0$ and end when the supersaturation reaches 90% of its final value; that is, when $S(y=0)=0.9S_M$.

To calculate t_R, the vapor pressure and temperature distributions derived above are used in (3), together with an expression for $p_e(T)$ taken from the *Smithsonian Meteorological Tables* (1951). The values used for α and D are 0.219 cm^2 sec^{-1} and 0.259 cm^2 sec^{-1}, respectively. Typical results for $d=1$ cm, $z_0=15$ cm are shown in Fig. 2, which shows values of t_R vs sample velocity for various values of (T_h-T_c).

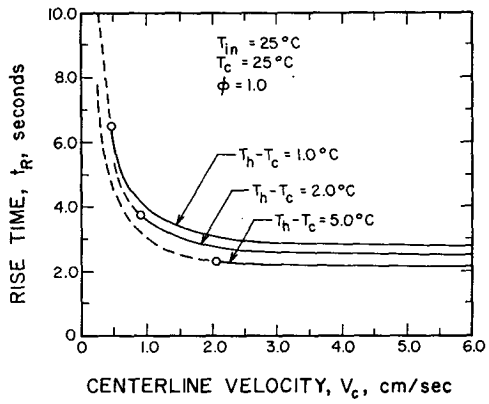

FIG. 2. Supersaturation rise time versus sample centerline velocity, for various values of T_h-T_c.

Fig. 2 illustrates clearly how longitudinal diffusion of heat and water vapor influences t_R.

Recall that the last term in (4) accounts for longitudinal diffusion of heat. Now consider transforming (4) so that time (t) is the independent variable, rather than z. Since z equals the product of velocity (u) and time, one then obtains

$$\frac{\partial T}{\partial t}=\alpha\left[\frac{\partial^2 T}{\partial y^2}+\left(\frac{\partial^2 T}{\partial t^2}\right)\Big/u^2\right], \quad (11)$$

where the last term is still the term accounting for longitudinal diffusion of heat. Clearly, as u becomes larger in (11), longitudinal diffusion of heat becomes less important. The same conclusion is valid for vapor diffusion because of the similarity of (4) and (7). After some thought, it becomes obvious that t_R should become insensitive to velocity for large enough velocities. This is evident in Fig. 2.

Hudson and Squires (1973) have given an expression for t_R based upon the assumption of negligible longitudinal diffusion. The values of t_R given in Fig. 2 for the region $u>3$ cm sec^{-1} agree with the Hudson-Squires expression to within 0.1 sec.

As the velocity is decreased below 3 cm sec^{-1}, Fig. 2 shows t_R increasing and, in the limit, going to infinity. This is due to the influence of longitudinal diffusion. To visualize why this is so, consider the case of very small u. In this case, the convective term (the first term) in (4) and (7) becomes negligible so that $T(y,z)$ and $p(y,z)$ become relatively insensitive to u. Thus, the length of the developing region becomes relatively insensitive to u. Since t_R equals this length divided by the centerline sample velocity, t_R goes to infinity as u approaches zero.

The reader will note a small circle on each of the curves in Fig. 2. These correspond to the condition given by (2), i.e., the limitation due to convection effects. Thus, the chamber should not be operated at sample velocities smaller than indicated by the circles.

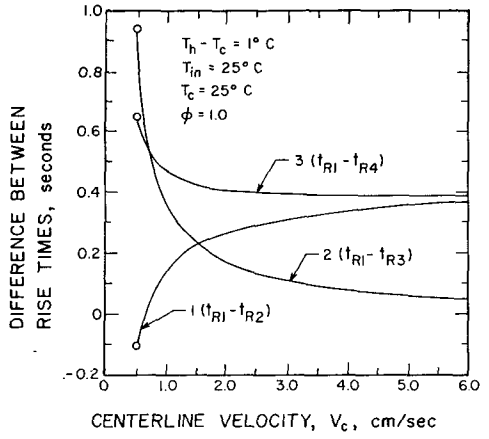

FIG. 3. Results of finite-difference calculations for $T_h - T_c = 1$C for values of t_{R1} obtained from Eq. (12). Curve 1 shows the influence of the velocity profile shape. Curve 2 indicates the influence of upstream longitudinal diffusion. Curve 3 shows both effects together.

Fig. 2 is specifically for $\phi = 1.0$, $T_{in} = T_c = 25$C. However, t_R is very insensitive to these conditions. For example, decreasing the inlet relative humidity from $\phi = 1.0$ to $\phi = 0.5$ increases the value of t_R by about 0.1 sec at 4.0 cm sec^{-1} and by a lesser amount at lower velocities. Regarding inlet temperature, decreasing T_{in} from 25 to 20C increases t_R by only 0.03 sec at 4.0 cm sec^{-1} and by an even smaller amount at lower velocities. Similarly, T_c has only an insignificant influence on t_R.

The above described insensitivity of t_R on ϕ and T_{in} indicates that the dry length of the hot plate is sufficiently long (15 cm) to assure that $p(y,z_0)$ is very close to p_c. Thus, the choice of p^* in Section 4 is not critical, and the values of t_R would be unaltered by taking $p^* = p_c$. The same conclusion will hold in general as long as $z_0 \geqslant 15d$. This generalization is apparent after noting in (6) and (9) that y and z are always divided by d. Since it is desirable that t_R be insensitive to ϕ and T_{in}, this conclusion is significant.

6. Simplified expression for t_R

The results shown in Fig. 2 are represented within 0.05 sec by the following simplified expression, which is derived by considering only the first term in the series solutions for p and T and by assuming $p^* = p_c$:

$$t_R = \tau \ln[950/(T_h - T_c)], \qquad (12)$$

where τ, the time constant, is given by

$$\tau = (2D/u^2)/\{[1 + 4\pi^2 D^2/(u^2 d^2)]^{\frac{1}{2}} - 1\}.$$

In view of the results of Section 5, Eq. (12) is valid for any chamber having a hot plate dry region of length $\geqslant 15$ times the plate spacing.

7. Finite-difference calculations

Two simplifying assumptions made in the above analyses seemed to merit further investigation.

Consider first the assumption of a constant sample velocity u across the gap between the plates. This "slug flow" assumption is clearly a simplification. In reality, the velocity must go to zero on approach to the walls because of viscous shear stresses. Also, the influence of upward buoyancy forces near the hot plate, and downward ones near the cold plate, make the downward velocity less near the hot plate than near the cold plate. Sinnarwalla and Alofs (1973) present a velocity profile which accounts for both viscous and buoyancy forces. This profile has the form of a third-order polynomial in y.

To investigate the importance of the slug flow assumption, finite-difference calculations were performed for the case $d = 1$ cm, $z_0 = 15$ cm. The appropriate techniques for this are presented by Collatz (1966) among others. Thus, Eqs. (4) and (5), (7) and (8), and (7) and (10) were numerically solved for specific values of $u(y)$ and specific values of T_h, T_c, T_{in} and ϕ. The values of t_R thus calculated are designated t_{R2}, while the value of t_R given by (12) for the same centerline velocity is designated t_{R1}. Curve 1 in Fig. 3 shows values of $(t_{R1} - t_{R2})$ for $(T_h - T_c) = 1$C and various sample velocities larger than indicated by (2). It can be seen that t_{R1} (slug flow) is almost always larger than t_{R2} (third-order velocity profile). A similar result is seen in Fig. 4 for $T_h - T_c = 5$C. Here the minimum sample velocity is 2.15 cm sec^{-1} in accord with (2).

Now consider another simplification which is made in Sections 2, 3 and 4. The third boundary condition in Eqs. (5) and (8) imply that the $z < 0$ region is unaffected by conditions in the $z > 0$ region. Thus, we have artificially delayed the process of the sample coming into vapor and temperature equilibrium with the hot plate and cold plate. This implies that t_R will be even less sensitive to T_{in} and ϕ than indicated in Section 5, and we may conclude that the simplification made in the third boundary condition in (5) and (8) are inconsequential.

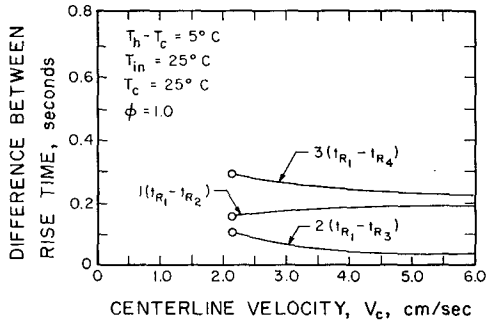

FIG. 4. As in Fig. 3 except for $T_h - T_c = 5$C.

The simplification made between the $z<15$ cm region and the $z>15$ cm region is of a similar nature. The third boundary condition in (10) artificially prevents the $z>15$ cm region from influencing the $z<15$ cm region. This simplification, which we entitle "neglect of upstream diffusion," is expected to cause an overestimate of t_R; but it seemed desirable to calculate the magnitude of the effect. Therefore, finite-difference numerical calculations were performed in such a way that the $z<15$ cm region influenced, and was influenced by, the $z>15$ cm region. Thus, Eq. (7) was numerically solved with the boundary conditions

$$\left.\begin{aligned} &p(-d/2,z)=p_c \\ &\frac{\partial p}{\partial y}(d/2,z<15\text{ cm})=0 \\ &p(d/2,z>15\text{ cm})=p_h \\ &p(y,0)=p_c \\ &p(y,z^*)=(p_c+p_h)/2+(y/d)(p_h-p_c) \end{aligned}\right\}, \qquad (13)$$

where $(z^*-15$ cm$)$ equals the product of t_R in (12) times the centerline sample velocity (V_c). Larger values for z^* took more computer time and were found to give the same result.

Let the t_R obtained by solving (7) and (13) with the slug flow assumption be designated t_{R3} and that obtained with the third-order velocity profile be designated t_{R1}. The latter is the more realistic rise time, but t_{R3} is also calculated in order to separate the effect of upstream diffusion from the effect of the shape of the velocity profile. Also, let t_{R1} be obtained from (12) for the same centerline velocity used to calculate t_{R3} and t_{R4}. Values of $(t_{R1}-t_{R3})$ and $(t_{R1}-t_{R4})$ are shown by curves 2 and 3, respectively, in Figs. 3 and 4: Fig. 3 is for $T_h-T_c=1$C and Fig. 4 for $T_h-T_c=5$C. Not surprisingly, it turns out that curve 3 in Figs. 3 and 4 is qualitatively equal to the addition of curves 1 and 2. This indicates that the effect of the velocity profile shape (curve 1) and upstream longitudinal diffusion (curve 2) approximately superpose.

In summary, the finite-difference calculations indicate that (12) overestimates t_R by 0.3–0.7 sec over a considerable operating range of the present chamber. In most applications this error will be negligible. We therefore conclude that the simplifying assumptions regarding velocity profile shape and longitudinal diffusion do not produce significant errors in (12). The finite-difference calculations are done for $d=1$ cm, $z_0=15$ cm, but the conclusion concerning the validity of (12) is expected to apply to any chamber having $z_0\geqslant 15d$.

8. Conclusions

The supersaturation rise time for steady-flow thermal diffusion chambers, either horizontal or vertical, should be calculated while taking longitudinal diffusion into account. The expression for t_R given in (12) adequately does this.

By providing such chambers with a dry region on the hot plate of length at least 15 times the plate spacing, the supersaturation rise time becomes relatively insensitive to the inlet sample humidity and temperature.

Acknowledgment. This work was supported by the Atmospheric Sciences Section, National Science Foundation, under Grant GA-30876.

REFERENCES

Carslaw and Jaeger, 1959: *Conduction of Heat in Solids*, 2nd. ed. Oxford University Press, 510 pp.

Collatz, L., 1966: *The Numerical Treatment of Differential Equations*, 3rd. ed. Berlin, Springer Verlag, 344–348.

Fitzgerald, J. W., 1970: Non-steady-state supersaturations in thermal diffusion chambers. *J. Atmos. Sci.*, **27**, 70–72.

——, 1972: On the computation of steady-state supersaturations in thermal diffusion chambers. *J. Atmos. Sci.*, **4**, 779–781.

Hudson, J., and P. Squires, 1973: Evaluation of a recording continuous cloud nucleus counter. *J. Appl. Meteor.*, **12**, 175–183.

Saxena, V. K., J. N. Burford and J. L. Kassner, Jr., 1970: Operation of a thermal diffusion chamber for measurements on cloud condensation nuclei. *J. Atmos. Sci.*, **27**, 73–80.

Schneider, P. J., 1957: Effect of axial fluid conduction on heat transfer in entrance regions of parallel plates and tubes. *Trans. ASME*, **79**, 765–773.

Sinnarwalla, A. M., and D. J. Alofs, 1973: A cloud nucleus counter with long available growth time. *J. Appl. Meteor.*, **12**, 831–835.

Smithsonian Meteorological Tables, 1951: R. J. List, Ed., 6th rev. ed., Washington, D. C.